Inorg. Chem. **2006**, *45*, 9123–9131

Rhodium Dimers with 2,2-Dimethyl-1,3-diisocyano and Bis(diphenylphosphino)methane Bridging Ligands

Justin J. Stace, Kurt D. Lambert, Jeanette A. Krause, and William B. Connick*

Department of Chemistry, P.O. Box 210172, University of Cincinnati, Cincinnati, Ohio 45221-0172

Received May 26, 2006

Four rhodium dimers have been synthesized with a bridging diisocyanide ligand, dmb (2,2-dimethyl-1,3-diisocyanopropane): $[Rh_2(dmb)_4](BPh_4)_2$, $[Rh_2(dmb)_4Cl_2]Cl_2$, $[Rh_2(dmb)_4I_2](PF_6)_2$, and $[Rh_2(dmb)_2(dppm)_2](BPh_4)_2$ (dppm = bis(diphenylphosphino)methane). The complexes have been characterized by elemental analysis and mass spectrometry, as well as UV–visible, IR, and ^{1}H NMR spectroscopies. X-ray crystal structures of the rhodium(I) complexes, $[Rh_2(dmb)_4](BPh_4)_2\cdot 1.5CH_3CN$ (3.2330(4), 3.2265(4) Å) and $[Rh_2(dmb)_2(dppm)_2](BPh_4)_2\cdot 0.5CH_3OH\cdot 0.2H_2O$ (3.0371(5) Å), confirm the existence of short Rh···Rh interactions. The metal–metal separation for the rhodium(II) adduct, $[Rh_2(dmb)_4Cl_2]Cl_2\cdot 6CHCl_3$ (2.8465(6) Å), is consistent with a formal Rh–Rh bond. For the two luminescent rhodium(I) dimers and six previously investigated diisocyano-bridged dimers with and without dppm ligands, the intense spin-allowed d$\sigma^*\rightarrow$pσ absorption band maximum shifts to longer wavelengths with decreasing Rh···Rh separation, and there is an approximate correlation between band energy and the inverse of the metal–metal separation cubed. Both $[Rh_2(dmb)_4]^{2+}$ and $[Rh_2(dmb)_4(dppm)_2]^{2+}$ undergo oxidative addition in the presence of iodine. In the conversion of $[Rh_2(dmb)_4]^{2+}$ to $[Rh_2(dmb)_4I_2]^{2+}$, the observed intermediate is tentatively assigned to a tetramer composed of two rhodium dimers. In the case of $[Rh_2(dmb)_2(dppm)_2]^{2+}$, no intermediate was detected.

Introduction

Rhodium(I) dimers with bridging diisocyanide ligands have been extensively investigated because of their rich thermal chemistry, photochemistry, and spectroscopy.[1−9] The bridging ligand scaffold holds the square planar metal centers in a face-to-face arrangement. As a consequence, the visible absorption spectra are typically dominated by an intense d$\sigma^*\rightarrow$pσ transition, where the filled dσ^* and unoccupied pσ orbitals derive from the interaction of orbitals on the two rhodium centers. For example, the most widely studied of these systems is $Rh(diprop)_4^{2+}$ (diprop = 1,3-diisocyanopropane), which exhibits a d$\sigma^*\rightarrow$pσ transition at 553 nm (14500 M^{-1} cm^{-1}) in acetonitrile solution.[10] Surprisingly, despite intense interest in the chemistry of these systems, there are only six different rhodium(I) dimers with bridging diisocyanide ligands that have been structurally characterized.

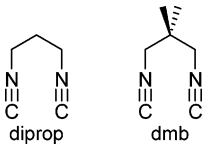

Inspired by the elegant studies of the multielectron reactivity of rhodium(I) dimers carried out by Hill and

* To whom correspondence should be addressed. E-mail address: bill.connick@uc.edu.

(1) Lewis, N. S.; Mann, K. R.; Gordon, J. G., II.; Gray, H. B. *J. Am. Chem. Soc.* **1976**, *98*, 7461−7463.
(2) Mann, K. R.; Lewis, N. S.; Miskowski, V. M.; Erwin, D. K.; Hammond, G. S.; Gray, H. B. *J. Am. Chem. Soc.* **1977**, *99*, 5525−5526.
(3) Mann, K. R.; Bell, R. A.; Gray, H. B. *Inorg. Chem.* **1979**, *18*, 2671−2673.
(4) Miskowski, V. M.; Sigal, I. S.; Mann, K. R.; Gray, H. B.; Milder, S. J.; Hammond, G. S.; Ryason, P. R. *J. Am. Chem. Soc.* **1979**, *101*, 4383−4385.
(5) Yaneff, P. V.; Powell, J. *J. Organomet. Chem.* **1979**, *179*, 101−113.
(6) Fukuzumi, S.; Nishizawa, N.; Tanaka, T. *Bull. Chem. Soc. Jpn.* **1983**, *56*, 709−714.
(7) Che, C. M.; Lee, W. M.; Kwong, H. L.; Yam, V. W. W.; Cho, K. C. *J. Chem. Soc., Dalton Trans.* **1990**, 1717−1722.
(8) Hill, M. G.; Mann, K. R. *Catal. Lett.* **1991**, *11*, 341−347.
(9) Coppens, P.; Gerlits, O.; Vorontsov, I. I.; Kovalevsky, A. Y.; Chen, Y.-S.; Graber, T.; Gembicky, M.; Novozhilova, I. V. *Chem. Commun.* **2004**, 2144−2145.
(10) Mann, K. R.; Thich, J. A.; Bell, R. A.; Coyle, C. L.; Gray, H. B. *Inorg. Chem.* **1980**, *19*, 2462−2468.

10.1021/ic060923g CCC: $33.50 © 2006 American Chemical Society
Published on Web 09/28/2006

Mann[11,12] and because of our interest in cooperative two-electron-transfer reactions,[13] we have undertaken the synthesis of two rhodium(I) complexes with a new ligand, 2,2-dimethyl-1,3-diisocyanopropane (dmb), and investigated the oxidative addition chemistry of these compounds. At the outset, it was our expectation that the methyl groups of dmb would yield samples that are more suitable for single-crystal X-ray diffraction studies than sometimes encountered with diprop. In this report, we describe the preparation, structures, and spectroscopy of a series of new rhodium dimers, including $[Rh_2(dmb)_2(dppm)_2](BPh_4)_2$, which exhibits a Rh···Rh separation that is shorter than previously reported for any rhodium(I) dimers with diisocyanide bridging ligands.

Experimental Section

1,5-Cyclooctadiene (COD) and 2,2-dimethyl-1,3-diaminopropane were obtained from Aldrich. $[Rh(COD)Cl]_2$ was prepared from $RhCl_3 \cdot 3H_2O$ (Pressure Chemicals), as described by Giordado and Crabtree.[14] All other reagents were obtained from Acros. Deuterated solvents for NMR spectroscopy were obtained from Cambridge Isotopes. Acetonitrile, dichloromethane, and chloroform were distilled from calcium hydride under argon, all other solvents used for synthesis were saturated with argon prior to use.

Elemental analyses on C, H, and N were performed by Atlantic Microlab, Inc. (Norcross, GA). ^{1}H NMR spectra were recorded using a Bruker AC-250 instrument and are referenced in ppm vs TMS. IR spectra were collected with a BioRad Excalibur spectrometer. UV−visible absorption spectra were recorded using either a HP-8453 diode array spectrophotometer or a fiber-optic dip probe attached to an Ocean Optics 2000CG CCD camera with a Mikropack DH-2000 UV−vis−NIR light source. Steady-state emission data were collected using a Fluorolog-3 fluorimeter. Emission samples for lifetime measurements were excited using 4−6 ns pulses from a Continuum Panther optical parametric oscillator, pumped with the third harmonic (355 nm) of a Surelite II Nd:YAG laser. Emission transients were detected with a modified PMT connected to a Tektronix TD5580D oscilloscope and modeled using in-house software on a Microsoft Excel platform. Mass spectra were obtained by high-resolution electrospray ionization using an Ionspec HiRes ESI−FTICRMS instrument. Observed isotope patterns were in excellent agreement with those calculated on the basis of natural isotopic abundances.

2,2-Dimethyl-1,3-diisocyanopropane (dmb). [***CAUTION:*** *Diisocyano ligands are potentially explosive when heated and should be handled with care!*] The ligand was prepared following a modification of the method reported by Ugi et al. for the preparation of alkyl isocyanides.[15] 2,2-Dimethyl-1,3-diaminopropane (5.19 g, 50.8 mmol) and benzyltriethylammonium chloride (0.253 g, 1.11 mmol) were dissolved in a mixture of 32 mL of chloroform and dichloromethane (25 mL), and an aqueous solution of saturated sodium hydroxide (30 mL) was added with vigorous stirring. The mixture was refluxed overnight. The reaction was quenched by addition of 170 mL of water. An attempt to purify the related diprop adduct by distillation resulted in a violent exothermic reaction. For this reason, the following procedure was adopted for isolation of dmb. The organic layer was first washed with a saturated NaCl solution (3 × 50 mL), and then it was washed with a sodium phosphate monobasic solution (3 × 50 mL) buffered to pH 5.5. The volume was reduced to approximately 10 mL, and the oily solution was dried over K_2CO_3. The product was dissolved in carbon tetrachloride, and the yield (12.2%) and concentration were estimated by ^{1}H NMR spectroscopy ($CDCl_3$) using a sample spiked with a known quantity of benzene. ^{1}H NMR ($CDCl_3$) δ (ppm): 1.14 (6H, s), 3.36 (4H, s).

$[Rh_2(dmb)_4](BPh_4)_2$. A slight molar excess of dmb (8.4 mL of a 1.2 M solution, 10.3 mmol) was added dropwise to an orange solution of $[Rh(COD)Cl]_2$ (1.25 g, 2.54 mmol) in 40 mL of chloroform. The resulting intense violet solution was refluxed overnight in the dark under argon. After cooling, a violet solid was collected by vacuum filtration and washed three times with 1.5 mL aliquots of $CHCl_3$, CH_2Cl_2, and diethyl ether. The deep violet powder was dried under vacuum to give (1.26 g, 65% yield) of $[Rh_2(dmb)_4]Cl_2$. The solid (0.167 g, 0.218 mmol) was dissolved in 50 mL of 90:10 methanol/water. A slight stoichiometric excess of $NaBPh_4$ (0.165 g, 0.482 mmol) in 90:10 methanol/water was added, and the solution was stirred at 40 °C under argon for 12 h. The crude tetraphenyl borate salt was collected by filtration and repeatedly washed with 90:10 methanol/water until the washings were colorless. Recrystallization by vapor diffusion of diethyl ether into an acetonitrile solution gave dark blue crystals (0.208 g, 72%). Anal. Calcd for $C_{76}H_{80}N_8B_2Rh_2 \cdot 1.5CH_3CN$: C, 68.04; H, 6.11; N, 9.54. Found: C, 67.70; H, 6.17; N, 8.66. ^{1}H NMR (d_6-DMSO) δ (ppm): 1.11 (24H, s, CH_3), 3.88 (16H, s, CH_2), 6.79 (8H, t, BPh_4 CH), 6.92 (16H, dd, BPh_4 CH), 7.18 (16H, br, s, BPh_4 CH). MS-ESI (*m*/*z*): 347.077 ($[Rh_2(dmb)_4]^{2+}$), 1313.297 ($[Rh_2(dmb)_4](BPh_4)^+$). IR (KBr pellet): 2176 cm^{-1}.

$[Rh_2(dmb)_4Cl_2]Cl_2$. $[Rh_2(dmb)_4]Cl_2$ (0.1941 g, 0.253 mmol) was dissolved in 35 mL of 6 M hydrochloric acid at 80 °C with vigorous stirring. Bubbling the dark blue solution with $Cl_{2(g)}$ for 5 min caused the color to change to green and then yellow. [***CAUTION:*** *Chlorine saturated 6 M HCl is extremely corrosive and should be handled with care!*]. The solution was filtered hot, yielding a yellow filtrate that was evaporated to dryness. The residue was dissolved in a minimal volume of acidic methanol (∼30 mM HCl), and diethyl ether was added to precipitate the product. After filtration, the solid was dissolved in acidic methanol, and *n*-propanol was added to induce precipitation. The yellow product was washed with ethanol and diethyl ether, (0.1037 g, 49.0% yield). ^{1}H NMR (d_6-DMSO) δ (ppm): 1.16 (24H, s, CH_3), 4.28 (16H, s, CH_2). MS-ESI (*m*/*z*): 347.1 ($[Rh_2(dmb)_4]^{2+}$), 383.1 ($[Rh_2(dmb)_4Cl_2]^{2+}$), 729.2 ($[Rh_2(dmb)_4]Cl^+$), 801.2 ($[Rh_2(dmb)_4Cl]Cl^+$). IR (KBr pellet): 2237 cm^{-1}.

$[Rh_2(dmb)_4I_2](PF_6)_2$. $[Rh_2(dmb)_4]Cl_2$ (0.072 g, 0.0932 mmol) was dissolved in ∼40 mL of hot methanol and filtered. The filtrate was purged with argon, and 8.4 mL of 0.0119 M (0.100 mmol) iodine in methanol was added with stirring. The solution was refluxed for 1.5 h, and the color changed from opaque violet to light brown. The solution was cooled to room temperature, and an aqueous solution of NH_4PF_6 (0.17 g in 7 mL) was added to give a brown-green precipitate. The resultant mixture was stirred for 10 min, cooled in ice, and filtered. The green-brown product was washed with cold 90:10 H_2O/CH_3OH and benzene until the filtrate was colorless. The solid was dried under vacuum to yield 0.071 g of crude product (61%). The product was purified by chromatography (Whatman chromatography paper; 5:20:75 CH_3CN/MeOH/CH_2Cl_2); the fast moving orange band afforded the product as an orange solid. Anal. Calcd for $C_{28}H_{40}N_8I_2P_2F_{12}Rh_2$: C, 27.16; H, 3.26; N, 9.05. Found: C, 27.53, H, 3.37; N, 8.71. ^{1}H NMR (d_6-

(11) Hill, M. G.; Mann, K. R. *Inorg. Chem.* **1991**, *30*, 1429−1431.
(12) Hill, M. G.; Mann, K. R. *Inorg. Chim. Acta* **1996**, *243*, 219−228.
(13) Jude, H.; Krause Bauer, J. A.; Connick, W. B. *J. Am. Chem. Soc.* **2003**, *125*, 3446−3447.
(14) Giordano, G.; Crabtree, R. H. *Inorg. Synth.* **1990**, *28*, 88−90.
(15) Weber, W. P.; Gokel, G. W.; Ugi, I. K. *Angew. Chem., Int. Ed. Engl.* **1972**, *11*, 530−531.

DMSO) δ (ppm): 1.12 (24H, s, CH_3), 4.19 (16H, s, CH_2). MS-ESI (*m*/*z*): 346.99 ($[Rh_2(dmb)_4]^{2+}$), 474.89 ($[Rh_2(dmb)_4I_2]^{2+}$), 1092.67 ($[Rh_2(dmb)_4I_2](PF_6)^+$. IR (KBr pellet): 2211 cm^{-1}.

$[Rh_2(dmb)_2(dppm)_2](BPh_4)_2$. To an orange solution of $[Rh(CO)(dppm)Cl]_2$ (0.0867 g, 0.122 mmol)[16] in 20 mL of 60:40 methanol/ethanol solution was added 170 μL of a 1.5 M solution of dmb (0.26 mmol) in CCl_4. The resulting dark violet solution was stirred at room temperature for 30 min. Addition of 3.0 mL of a ~0.150 M solution of $NaBPh_4$ (0.45 mmol) afforded a turquoise blue precipitate, and the mixture was stirred overnight. The blue product was collected by vacuum filtration and washed with hexanes, chloroform, 80:20 MeOH/H_2O, and diethyl ether. The product was dried overnight under vacuum (0.0991 g, 47.3% yield). ^{1}H NMR (d_6-DMSO) δ (ppm): 0.105 (12H, s, CH_3, dmb), 2.95 (8H, s, CH_2, dmb), 4.45 (4H, s, CH_2, dppm), 6.78 (8H, t, BPh_4^-), 6.92 (16H dd, BPh_4^-), 7.16 (16H, br, s, BPh_4^-), 7.45 (24H, br, s dppm), 8.00 (16H, s, dppm). ^{31}P NMR (CD_3CN) δ (ppm): 24.6 (d). MS-ESI (*m*/*z*): 478.1 ($[Rh_2(dmb)_2(dppm)(PPhCH_2)]^{2+}$), 609.0 [$(Rh_2(dmb)_2(dppm)_2]^{2+}$), 1537.4 ($[Rh_2(dmb)_2(dppm)_2](BPh_4)^+$). IR (KBr pellet): 2164 cm^{-1}.

X-ray Crystallography. Blue needles of $[Rh_2(dmb)_4](BPh_4)_2 \cdot 1.5CH_3CN$ were obtained by vapor diffusion of diethyl ether into an acetonitrile solution. Yellow needles of $[Rh_2(dmb)_4Cl_2]Cl_2 \cdot 6CHCl_3$ were grown from an acetonitrile solution layered over chloroform. Blue needles of $[Rh_2(dmb)_2(dppm)_2](BPh_4)_2 \cdot 0.5CH_3OH \cdot 0.2H_2O$ were grown by vapor diffusion of diethyl ether into an acetonitrile solution of $[Rh_2(dmb)_2(dppm)_2](BPh_4)_2$.

Data for crystal structures were collected at 150 K using a standard Bruker SMART 1K CCD diffractometer with graphite-monochromated Mo Kα radiation ($\lambda = 0.71073$ Å). The data frames were processed using the program SAINT[17] and corrected for decay, Lorentz, and polarization effects. Absorption and beam corrections based on the multiscan technique were applied using SADABS.[18] The structures were solved by a combination of direct methods and the difference Fourier technique, and the resulting models were refined by full-matrix least squares on F^2 using SHELXTL.[19] Non-hydrogen atoms were refined with anisotropic displacement parameters. All hydrogen atoms were either located on the difference map or calculated on the basis of geometric criteria and treated with a riding model. The isotropic temperature factors for the H-atoms were defined as *a* times U_{eq} of the adjacent atom where $a = 1.5$ for methyl and hydroxyl hydrogens and 1.2 for all others. For crystals of $[Rh_2(dmb)_4](BPh_4)_2 \cdot 1.5CH_3CN$, one CH_3CN molecule behaves nicely, whereas the other is disordered and has an occupancy of 50%. The $[Rh_2(dmb)_2(dppm)_2](BPh_4)_2$ molecule crystallizes with a disordered, partially occupied methanol (50% occupancy) and water (20% occupancy).

Results and Discussion

Synthesis and Characterization. Drawing on the work of Mann, Lewis, Gray, and Powell[1,5] we have prepared a series of rhodium dimers with a new diisocyano-bridging ligand, dmb. The deep violet chloride salt of $Rh_2(dmb)_4^{2+}$ was prepared by slow addition of dmb to a dilute chloroform solution of $[Rh(COD)Cl]_2$. The tetraphenylborate salt was isolated by anion metathesis, and analytical grade material was obtained by vapor diffusion of diethyl ether into a concentrated acetonitrile solution. The formally rhodium(I) dimer was oxidized to the yellow dichloro adduct, $Rh_2(dmb)_4Cl_2^{2+}$, upon exposure to chlorine-saturated, hot 6 M HCl solution. Similarly, $Rh_2(dmb)_4^{2+}$ in methanol reacts with 1 equiv of iodine to give the corresponding diiodo rhodium(II) adduct, $Rh_2(dmb)_4I_2^{2+}$, which is readily isolated by chromatography as the orange hexafluorophosphate salt. We also have observed that addition of more than 4 molar equiv of iodine produces a sparingly soluble green product. On the other hand, the heteroleptic system, $Rh_2(dmb)_2(dppm)_2^{2+}$, was prepared in high yield from the reaction of $[Rh(CO)(dppm)Cl]_2$ with dmb; anion metathesis afforded the deep turquoise tetraphenylborate salt. The product is air-sensitive in fluid solution.

The compositions of the four salts were verified by elemental analysis. In addition, each complex gave rise to an ESI mass spectrum with dominant peaks consistent with a +2 charged dimer and a +1 charged dimer with one counteranion, confirming the formulation of these compounds as binuclear complexes. The solution ^{1}H NMR spectra are consistent with diamagnetic products having symmetrical bridging diisocyanide ligands. For example, $Rh_2(dmb)_4^{2+}$ in d_6-DMSO exhibits two singlet resonances in an approximate 3:2 intensity ratio at 1.11 and 3.88 ppm, respectively. Thus, each four-coordinate metal center of $Rh_2(dmb)_4^{2+}$ has eight paired valence 4d electrons, as expected for a d^8-d^8 dimer. The corresponding resonances for the dichloro adduct (1.16, 4.28 ppm) are shifted downfield from those of the parent complex, as expected for reduced electron density on the rhodium(II) centers of a d^7-d^7 dimer. The shift is smaller for $[Rh_2(dmb)_4I_2](PF_6)_2$ (1.12, 4.19 ppm), reflecting the relative electron donor capacities of chloride and iodide ligands. In contrast, the dmb methyl and methylene resonances for $[Rh_2(dmb)_2(dppm)_2](BPh_4)_2$ (0.11, 2.95 ppm) are shifted substantially upfield from those of the free ligand (1.02, 3.23 pm) as a consequence of shielding by the nearby dppm phenyl groups (vide infra); we suggest that a similar explanation may account for substantial shielding of some isocyanide ligand protons of $Rh_2(dimen)_2(dppm)_2^{2+}$ (0.3−1.6 ppm; dimen = 1,8-diisocyano-*p*-menthane).[20] By contrast, the dppm methylene resonance for $Rh_2(dmb)_2(dppm)_2^{2+}$ is shifted significantly downfield from that of the free ligand (2.97 ppm) to 4.45 ppm.

The infrared spectrum of each salt has a strong band near 2200 cm^{-1}, attributed to the dmb C≡N stretch. For $[Rh_2(dmb)_4](BPh_4)_2$ in a KBr matrix, the maximum (2176 cm^{-1}) is in excellent agreement with that observed for $[Rh_2(diprop)_4](BPh_4)_2 \cdot 2CH_3CN$ (2172 cm^{-1}).[1] The band is shifted to lower frequency for $[Rh_2(dmb)_2(dppm)_2](BPh_4)_2$ (2164 cm^{-1}), in keeping with the comparatively weaker π-back-

(16) Kubiak, C. P.; Eisenberg, R. *Inorg. Chem.* **1980**, *19*, 2726−2732.
(17) Bruker SMART v5.051 and SAINT v5.A06 programs were used for data collection and data processing, respectively. *SMART v5.051*; *SAINT v5.A06*; Bruker Analytical X-ray Instruments, Inc.: Madison WI.
(18) SADABS v2.10 was used for the application of semiempirical absorption and beam corrections. Sheldrick, G. M. *SADABS v2.10*; University of Göttingen: Göttingen, Germany.
(19) SHELXTL v5.03, 6.1, and 6.14 were used for the structure solution and generation of figures and tables. Neutral-atom scattering factors were used as stored in this package. Sheldrick, G. M. *SHELXTL v5.03, 6.1, and 6.14*; University of Göttingen: Göttingen, Germany; Bruker Analytical X-ray Solutions, Inc.: Madison, WI.
(20) Boyd, D. C.; Matsch, P. A.; Mixa, M. M.; Mann, K. R. *Inorg. Chem.* **1986**, *25*, 3331−3333.

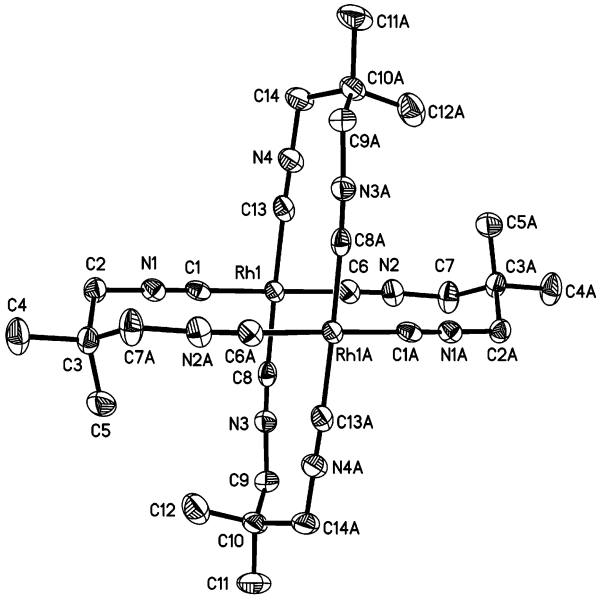

Figure 1. ORTEP diagram of one of the two independent dications of $[Rh_2(dmb)_4](BPh_4)_2 \cdot 1.5CH_3CN$ (50% ellipsoids). Hydrogen atoms, anions and solvent have been omitted for clarity.

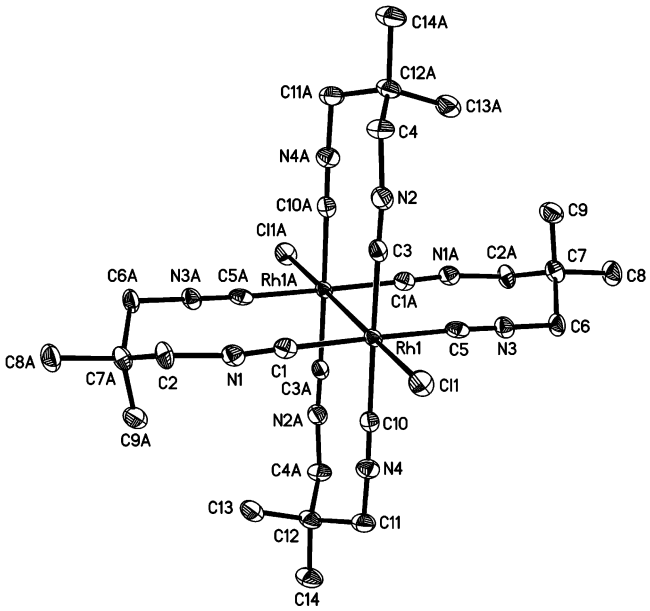

Figure 2. ORTEP diagram of $[Rh_2(dmb)_4Cl_2]Cl_2 \cdot 6CHCl_3$ (50% ellipsoids). Hydrogen atoms, anions, and solvent have been omitted for clarity.

bonding character of the dppm ligand. Because of the reduced electron density on the metal centers of the d^7-d^7 complexes, the maximum occurs at higher frequencies for the dichloro and diiodo adducts (Cl, 2237 cm^{-1}; I, 2211 cm^{-1}); the values for the latter two complexes are consistent with the relative electron-releasing properties of the halide ligand.[21]

X-ray Crystallography. The structures of three of the dimers were confirmed by single-crystal X-ray diffraction studies at 150 K. ORTEP diagrams are shown in Figures 1−3, and relevant data are summarized in Tables 1−3. In each case, the anions, dications, and solvent pack as discrete

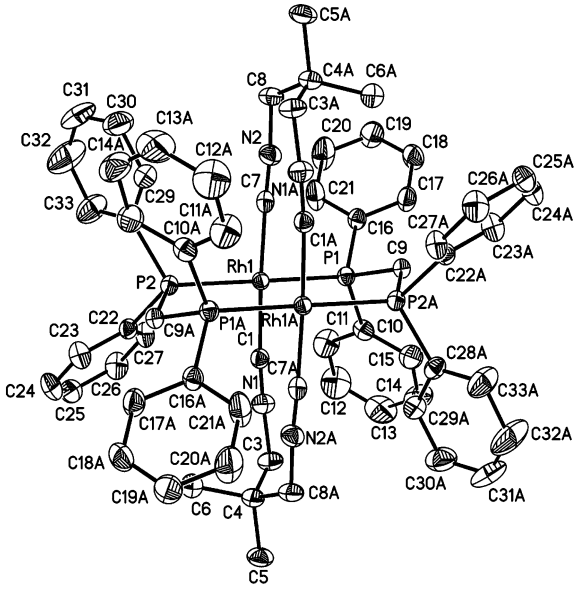

Figure 3. ORTEP diagram of $[Rh_2(dmb)_2(dppm)_2](BPh_4)_2 \cdot 0.5CH_3OH \cdot 0.2H_2O$ (50% ellipsoids). Hydrogen atoms, anions, and solvent have been omitted for clarity.

molecules, and there are no unusually short intermolecular contacts.

$[Rh_2(dmb)_4](BPh_4)_2 \cdot 1.5CH_3CN$ crystallizes as two independent molecules in the asymmetric unit, with each complex lying on a center of inversion. The dications exhibit the characteristic paddle-wheel structure associated with diisocyano-bridged rhodium dimers (Figure 1) in which the bridging dmb ligands hold the approximately square planar metal centers in a nearly eclipsed face-to-face arrangement. The formally nonbonding intramolecular Rh···Rh contacts (3.2330(4) and 3.2265(4) Å) fall within the 3.222−3.296 Å range reported for five structures of $Rh_2(diprop)_4^{2+}$.[10,22] In each independent molecule, the Rh centers are displaced just slightly away from one another, with Rh1 and Rh2 lying 0.040 and 0.032 Å, respectively, out of the coordination plane defined by the four bonded carbon atoms. The center methylene carbon of the dmb backbone is folded toward one adjacent dmb ligand and away from the other. This carbon atom is well-ordered, and it seems probable that the attached methyl groups help to avoid the disorder problem commonly encountered with the center methylene group of diprop.[10,22] In keeping with computational and experimental results for $Rh(diprop)_4^{2+}$,[10,22,23] $Rh_2(dmb)_4^{2+}$ favors a nearly eclipsed geometry with very small C−Rh···Rh−C twist angles (ω, 1.2(1)° and 0.5(1)° for Molecule A and 1.8(1)° and 0.9(1)° for Molecule B).

In crystals of $[Rh_2(dmb)_4Cl_2]Cl_2 \cdot 6CHCl_3$, each complex lies on an inversion center, adopting a paddle-wheel structure that is similar to that of the parent d^8-d^8 dication with small C−Rh−Rh−C twist angles (1.1(2)°, 0.8(2)°). However, the metal−metal separation (2.8465(6) Å) is considerably shorter, as expected for a formal metal−metal bonding interaction.

(21) Poulton, J. T.; Sigalas, M. P.; Folting, K.; Streib, W. E.; Eisenstein, O.; Caulton, K. G. *Inorg. Chem.* **1994**, *33*, 1476−1485.

(22) Gerlits, O.; Kovalevsky, A. Y.; Coppens, P. *J. Chem. Soc., Dalton Trans.* **2004**, 3955−3962.

(23) Novozhilova, I. V.; Volkov, A. V.; Coppens, P. *Inorg. Chem.* **2004**, *43*, 2299−2307.

Table 1. Crystal and Structure Refinement Data for $[Rh_2(dmb)_4](BPh_4)_2 \cdot 1.5CH_3CN$, $[Rh_2(dmb)_4Cl_2]Cl_2 \cdot 6CHCl_3$ and $[Rh_2(dmb)_2(dppm)_2](BPh_4)_2 \cdot 0.5CH_3OH \cdot 0.2H_2O$

	$[Rh_2(dmb)_4](BPh_4)_2 \cdot 1.5CH_3CN$	$[Rh_2(dmb)_4Cl_2]Cl_2 \cdot 6CHCl_3$	$[Rh_2(dmb)_2(dppm)_2](BPh_4)_2 \cdot 0.5CH_3OH \cdot 0.2H_2O$
empirical formula	$[C_{28}H_{40}N_8Rh_2][BC_{24}H_{20}]_2 \cdot 1.5CH_3CN$	$[C_{28}H_{40}Cl_2N_8Rh_2]Cl_2 \cdot 6CHCl_3$	$[C_{64}H_{64}N_4P_4Rh][BC_{24}H_{20}]_2 \cdot 0.5CH_3OH \cdot 0.2H_2O$
cryst syst	monoclinic	monoclinic	monoclinic
space group	$P2_1/c$	$C2/c$	$P2_1/n$
a (Å)	22.9710(4)	30.2025(16)	16.5108(2)
b (Å)	13.5778(1)	10.2584(6)	17.2821(3)
c (Å)	24.9004(5)	19.7543(6)	19.7071(4)
α (°)	90	90	90
β (°)	115.889(1)	100.906(2)	113.102(1)
γ (°)	90	90	90
V (Å^3), Z	6986.9(2), 4	6009.9(5), 4	5172.31(15), 2
reflns: coll./indep./R_{int}	44 832/17 115/0.0617	31 168/7341/0.0741	33 103/12 617/0.0538
params	843	298	559
R1/wR2 [$I > 2\sigma(I)$][a]	0.0436/0.0774	0.0485/0.1034	0.0537/0.1388
R1/wR2 (all data)[a]	0.0976/0.0919	0.0873/0.1171	0.1003/0.1585

[a] $R1 = \sum||F_o| - |F_c|/\sum|F_o|$; $wR2 = [\sum w(F_o^2 - F_c^2)^2/\sum w(F_o^2)^2]^{1/2}$.

Table 2. Selected Distances (Å) and Angles (deg) for $[Rh_2(dmb)_4](BPh_4)_2 \cdot 1.5CH_3CN$, $[Rh_2(dmb)_4Cl_2]Cl_2 \cdot 6CHCl_3$, and $[Rh_2(dmb)_2(dppm)_2](BPh_4)_2 \cdot 0.5CH_3OH \cdot 0.2H_2O$[a]

$[Rh_2(dmb)_4](BPh_4)_2 \cdot 1.5CH_3CN$		$[Rh_2(dmb)_4Cl_2]Cl_2 \cdot 6CHCl_3$		$[Rh_2(dmb)_2(dppm)_2](BPh_4)_2 \cdot 0.5CH_3OH \cdot 0.2H_2O$	
Rh(1)−Rh(1)#1	3.2330(4)	Rh(1)−Rh(1)#3	2.8465(6)	Rh(1)−Rh(1)#2	3.0371(5)
Rh(2)−Rh(2)#2	3.2265(4)	Rh(1)−C(1)	1.990(4)	Rh(1)−C(1)	1.945(4)
Rh(1)−C(1)	1.977(3)	Rh(1)−C(3)	1.975(4)	Rh(1)−C(7)	1.957(4)
Rh(1)−C(6)	1.966(3)	Rh(1)−C(5)	1.982(4)	Rh(1)−P(1)	2.3046(10)
Rh(1)−C(8)	1.982(3)	Rh(1)−C(10)	1.981(4)	Rh(1)−P(2)	2.3143(10)
Rh(1)−C(13)	1.965(3)	Rh(1)−Cl(1)	2.4467(11)		
Rh(2)−C(15)	1.964(3)			C(1)−Rh(1)−C(7)	177.04(15)
Rh(2)−C(20)#2	1.969(3)	C(1)−Rh(1)−C(5)	178.87(17)	P(1)−Rh(1)−P(2)	175.80(4)
Rh(2)−C(22)	1.977(3)	C(3)−Rh(1)−C(10)	179.15(17)	C(1)−Rh(1)−P(1)	89.35(11)
Rh(2)−C(26)	1.971(3)	C(1)−Rh(1)−C(3)	90.11(17)	C(1)−Rh(1)−P(2)	90.22(11)
		C(1)−Rh(1)−C(10)	90.73(16)	C(7)−Rh(1)−P(1)	87.75(11)
C(1)−Rh(1)−C(6)	177.46(12)	C(3)−Rh(1)−C(5)	91.00(16)	C(7)−Rh(1)−P(2)	92.72(11)
C(8)−Rh(1)−C(13)	177.64(12)	C(5)−Rh(1)−C(10)	88.16(16)		
C(1)−Rh(1)−C(8)	92.16(12)	C(1)−Rh(1)−Cl(1)	90.15(12)		
C(1)−Rh(1)−C(13)	88.18(13)	C(3)−Rh(1)−Cl(1)	89.91(12)		
C(6)−Rh(1)−C(8)	88.92(13)	C(5)−Rh(1)−Cl(1)	89.64(12)		
C(13)−Rh(1)−C(6)	90.65(14)	C(10)−Rh(1)−Cl(1)	90.21(11)		
C(15)−Rh(2)−C(20)#2	177.40(13)	Cl(1)−Rh(1)−Rh(1)#3	179.39(3)		
C(22)−Rh(2)−C(26)	177.87(13)				
C(15)−Rh(2)−C(22)	91.08(12)				
C(15)−Rh(2)−C(26)	88.00(12)				
C(20)#2−Rh(2)−C(22)	90.77(12)				
C(20)#2−Rh(2)−C(26)	90.10(12)				

[a] Symmetry operations: #1, $-x$,1 $-$ y, $-z$; #2, 1 $-$ x, 1 $-$ y, 1 $-$ z; #3, 1/2 $-$ x, 1/2 $-$ y, $-z$.

Table 3. UV−Visible Absorption and Emission Data for Rhodium Dimers

compound	absorption max, nm (ϵ M^{-1} cm^{-1})	emission max, nm
$[Rh_2(dmb)_4](BPh_4)_2$[a]	318 (35 900), 344 (5300), 560 (12 300)	663, >830
$[Rh_2(dmb)_4Cl_2]Cl_2$[b]	343 (21 900), 420sh (1200)	
$[Rh_2(dmb)_4I_2](PF_6)_2$[a]	321 (7000), 402 (29 300), 472 (11 000)	
$[Rh_2(dmb)_2(dppm)_2](BPh_4)_2$[a]	321 (19 100), 345sh (4000), 624 (15 300)	710

[a] Acetonitrile solution. [b] Methanol solution.

The Rh−Rh and axial Rh−Cl (2.447(1) Å) distances are nearly identical to those reported for $[Rh_2(diprop)_4Cl_2]Cl_2 \cdot 8H_2O$ (2.837(1), 2.447(1) Å; ω, 0°).[3] The arrangement of isocyanide groups around the Rh center results in an almost perfectly square planar coordination geometry with angular distortions from ideality of <2°. Because of the nearly eclipsed geometry, there are short intramolecular C···C and N···N (2.842(6)−2.877(5) Å) contacts between the isocyanide groups of the bridging ligand; comparable nonbonded *ipso* C···C distances (2.82 Å) have been found for [2.2]-paracyclophanes, which exhibit characteristic puckering of the phenylene groups to accommodate the constrained geometry.[24−26] In the present case, these steric interactions may account for slightly longer metal−metal distances than found for unsupported $[Rh_2(p\text{-}CH_3C_6H_4NC)_8I_2](PF_6)_2$ (2.785(2) Å),[27] as well as $[Rh_2(TMB)_4Cl_2](PF_6)_2$ (2.770(3) Å; TMB

(24) Hope, H.; Bernstein, J.; Trueblood, K. W. *Acta Crystallogr.* **1972**, *B28*, 1733−1743.
(25) Keehn, P. M. *Cyclophanes Vol 1*; Academic Press: New York, 1983; Vol. 1.
(26) Ball, P.; Shtoyko, T. R.; Krause Bauer, J. A.; Oldham, W. J.; Connick, W. B. *Inorg. Chem.* **2004**, *43*, 622−632.
(27) Olmstead, M. M.; Balch, A. L. *J. Organomet. Chem.* **1978**, *148*, C15−C18.

= 2,5-diisocyano-2,5-dimethylhexane),[28] which adopt a staggered geometry.[3] The dimers lie between layers of both anions and solvent parallel to the *bc* plane. Each chloride counterion is surrounded by three chloroform molecules that form short C−H···Cl interactions, as indicated by the C···Cl distances (C17···Cl11, 3.524(6); C15···Cl1, 3.545(6), C16···Cl11, 3.388(6) Å); there also are short intermolecular C6···Cl distances of 3.525(5) and 3.666(5) Å involving the counterion (Cl11) and chloride bonded to the rhodium center (Cl1), respectively.

In crystals of $[Rh_2(dmb)_2(dppm)_2](BPh_4)_2 \cdot 0.5CH_3OH \cdot 0.2H_2O$, each dimer is situated on an inversion center. The bridging ligand scaffold holds the roughly square planar metal center in a nearly eclipsed conformation with L−Rh···Rh−L torsional twist angles of 0.49(4)° and 2.9(2)° for the dppm and dmb ligands, respectively. The resulting 3.0371(5) Å metal−metal separation is the shortest that has been reported for rhodium(I) dimers with bridging phosphine and diisocyano ligands. For example, this distance is shorter than found for $[Rh_2(dimen)_2(dppm)_2](PF_6)_2$ (3.161(1) Å; ω, 0°),[20] as well as $[Rh_2(HTP5)_2(dppm)_2](PF_6)_2$ (3.070 Å; HTP5 = 1,5-diisocyano-1,1,5-triphenylpentane), for which steric demands of the HTP5 ligand are believed to account for the observed 26° twist angle (ω) and short metal−metal separation.[29] There are very small tetrahedral distortions at the metal, as indicated by the C−Rh−C (177.04(15)°) and P−Rh−P (175.80(4)°) bond angles; the P atoms of the same dppm ligand are shifted slightly away from each other (P···P, 3.205(1) Å), whereas the coordinated C atoms of the same dmb ligand are shifted very slightly toward each other (C···C, 3.025(5) Å). The center methylene carbons of the dmb and dppm ligands are folded toward each other, effectively projecting the C6 methyl group of the dmb ligand between two dppm phenyl rings (Figure 3). This relatively congested geometry results in short contacts between C6 and the ring centroids of the phenyl groups (C22 phenyl, 4.30 Å; C16A phenyl, 4.90 Å). There exist similar short C··· phenyl ring centroid distances for the dmb methylene carbons C6 (C10 phenyl, 4.06 Å; C22 phenyl, 4.97 Å) and C8 (C28 phenyl, 4.33 Å; C16 phenyl, 4.76 Å). Although the methyl protons of C5 and C6 are chemically equivalent on the NMR time scale (as are the methylene protons of C6 and C8), the existence of short interactions between these protons and the dppm phenyl rings likely accounts for the observed shielding in the ^{1}H NMR spectrum.

Electronic Spectroscopy. Given the structural similarities between this series of complexes and those with the diprop ligand, it is not surprising that the UV−visible absorption properties also are similar (Table 3). To a reasonable approximation, the electronic structures of this class of rhodium(I) dimers can be understood in terms of the strong interactions between the $4d_{z^2}$ and $5p_z$ orbitals of the two square planar metal centers held in a face-to-face arrangement.[1,30−32]

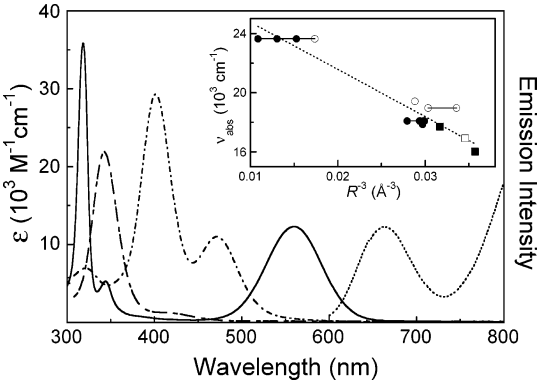

Figure 4. UV−visible absorption spectra of $[Rh_2(dmb)_4]^{2+}$ (—) and $[Rh_2(dmb)_4I_2]^{2+}$ in acetonitrile (— · —), as well as $[Rh_2(dmb)_4Cl_2]^{2+}$ in methanol (— — —). Emission spectrum (λ_{ex} = 560 nm) of $[Rh_2(dmb)_4]^{2+}$ in degassed acetonitrile (···). Inset shows d$\sigma^*\rightarrow$pσ absorption maximum (ν_{abs}) as a function of the inverse of the metal−metal separation cubed (R^{-3}) for eight structurally characterized diisocyanide-supported rhodium(I) dimers with (○, ●) and without (□, ■) dppm ligands: $[Rh_2(dimen)_4]^{2+}$ (0.0109−0.0174), $[Rh_2(TMB)_4]^{2+}$ (0.0288), $[Rh_2(diprop)_4]^{2+}$ (0.0293−0.0299), $[Rh_2(dmb)_4]^{2+}$ (0.0297), $[Rh_2(dihex)_4]^{2+}$ (dihex = 1,4-diisocyanohexane) (0.0303−0.0336), $[Rh_2(dimen)_2(dppm)_2]^{2+}$ (0.0317), $[Rh_2(HTP5)_2(dppm)_2]^{2+}$ (0.0346), $[Rh_2(dmb)_2(dppm)_2]^{2+}$ (0.0357).[10,20,22,29,35,37−39] For open points, $\omega > 10°$; for shaded points, $\omega < 10°$. Horizontal lines connect structures of the same complex with different anions. The dashed line shows linear best fit.

The occupied $4d_{z^2}$ levels split to give fully occupied bonding (dσ) and antibonding (dσ*) molecular orbitals. The unoccupied $5p_z$ levels split to give pσ and pσ* orbitals. Therefore, the intense band in the long-wavelength region of the electronic spectra of these compounds has been previously assigned to a spin-allowed d$\sigma^*\rightarrow$pσ transition.[1,10,33,34] In the case of the rhodium(II) halide dimers, the dσ level is occupied and the dσ* is unoccupied, resulting in a formal bond order of one; spectra of these complexes are dominated by an intense d$\sigma\rightarrow$dσ* transition. A refinement of this description takes into account symmetry-allowed mixing of the $5p_z$ orbital with the occupied $4d_{z^2}$ and low-lying unoccupied isocyanide π* levels.[10,23,32] A further perturbation considers the influence of rotameric conformation as measured by the ω twist angle.[9,10,35] Additionally, in the case of the rhodium(II) halide dimers, we can anticipate additional perturbation due to coupling of the d$\sigma\rightarrow$dσ* and axial halide-to-metal (X$\sigma\rightarrow$dσ*) charge-transfer transitions.[32]

In room-temperature acetonitrile solution, the d^8-d^8 dimers, $Rh_2(dmb)_4^{2+}$ and $Rh_2(dmb)_2(dppm)_2^{2+}$, exhibit intense spin-allowed d$\sigma^*\rightarrow$pσ bands maximizing at 560 and 630 nm, respectively, with comparable full-width-at-half-maximum values (fwhm: 2370, 1800 cm^{-1}) (Table 3, Figure 4). The ~2000 cm^{-1} stabilization for the dppm complex is qualitatively consistent with its shorter Rh···Rh separation (3.04 vs 3.23 Å) and the resulting enhanced orbital interac-

(28) Maverick, A. W.; Smith, T. P.; Maverick, E. F.; Gray, H. B. *Inorg. Chem.* **1987**, *26*, 4336−4341.
(29) Daws, C. A.; Hill, M. G.; Bullock, J. P.; Mann, K. R. *Inorg. Chem.* **1992**, *31*, 2948−2955.
(30) Mann, K. R.; Gordon, J. G., II.; Gray, H. B. *J. Am. Chem. Soc.* **1975**, *97*, 3553−3555.
(31) Mann, K. R.; DiPierro, M. J.; Gill, T. P. *J. Am. Chem. Soc.* **1980**, *102*, 2, 3965−3967.
(32) Miskowski, V. M.; Smith, T. P.; Loehr, T. M.; Gray, H. B. *J. Am. Chem. Soc.* **1985**, *107*, 7925−7934.
(33) Rice, S. F.; Miskowski, V. M.; Gray, H. B. *Inorg. Chem.* **1988**, *27*, 4704−4708.
(34) Recent computational results (ref 23), suggesting significant isocyanide contribution to the LUMO, are at odds with experiments that indicate minimal MLCT character in this excited state (ref 33).
(35) Exstrom, C. L.; Britton, D.; Mann, K. R.; Hill, M. G.; Miksowksi, V. M.; Schaefer, W. P.; Gray, H. B. *Inorg. Chem.* **1996**, *35*, 549−550.

tions between metal centers which destabilize the dσ^* orbital relative to the pσ level. Thus, $Rh_2(dmb)_2(dppm)_2^{2+}$ exhibits the longest wavelength d$\sigma^*\rightarrow$pσ transition of reported rhodium(I) dimers with bridging diisocyanide ligands.[5,7,12,20,29,36] The sensitivity of this transition to variation in metal−metal separation (R) also is suggested by comparison with the spectra of $Rh_2(HTP5)_2(dppm)_2^{2+}$ (591 nm in CH_2Cl_2; 3.070 Å)[29] and $Rh_2(dimen)_2(dppm)_2^{2+}$ (565 nm in CH_2Cl_2; 3.161(1) Å).[20] The inset in Figure 4 shows the d$\sigma^*\rightarrow$pσ solution absorption maximum (ν_{abs}, cm^{-1}) as a function of R^{-3} for eight structurally characterized diisocyanide-supported rhodium(I) dimers.[10,20,22,29,35,37−39] The plot illustrates the loose correlation between transition energy and metal−metal separation; the trend appears to hold despite the possibility that solution and solid-state structures may be somewhat different. Mann, Coppens, and co-workers have examined this issue and established that both metal−metal separation and twist angle significantly influence the energy of the d$\sigma^*\rightarrow$pσ transition.[22,23,31,35,40] In this regard, we note that complexes with larger twist angles (>10°) tend to deviate the most from the apparent relationship in Figure 4 by having larger (rather than smaller) ν_{abs} values. What we wish to point out here is that, although it is not necessarily to be expected, three diisocyanide-supported dimers with dppm ligands also follow the approximate dependence of ν_{abs} on metal−metal separation.

The spectra of the d^7-d^7 dimers with axial halide ligands are in reasonable agreement with those reported for the corresponding diprop complexes. $Rh_2(dmb)_4Cl_2^{2+}$ exhibits an intense d$\sigma\rightarrow$dσ^* transition maximizing at 343 nm (Figure 4). In accord with the description developed by Miskowski and co-workers,[32] the long-wavelength shoulder near 420 nm is assigned to the closely spaced d$\pi^*\rightarrow$dσ^* and d$\delta^*\rightarrow$dσ^* transitions, where the dπ^* and dδ^* orbitals result from metal−metal antibonding combinations of the $d_{xz,yz}$ and d_{xy} orbitals, respectively. The spectrum of the dibromo adduct, $Rh_2(dmb)_4Br_2^{2+}$, is qualitatively similar with the d$\sigma\rightarrow$dσ^* band maximizing near 370 nm.[41] However, the spectrum of $Rh_2(dmb)_4I_2^{2+}$ is characteristically different, showing *two* relatively intense absorption maxima (acetonitrile; 402, 472 nm). The red-shift of these bands from the d$\sigma\rightarrow$dσ^* transitions of dichloro and dibromo complexes is in keeping with the notion of mixing of the metal−metal d$\sigma\rightarrow$dσ^* and ligand-to-metal X$\sigma\rightarrow$dσ^* charge-transfer transitions. Miskowski and co-workers have suggested that the mixing is sufficiently strong in the case of axial iodide ligands that neither component can be regarded as having pure metal−metal or ligand-to-metal charge-transfer character.[32]

Emission Spectroscopy. Both d^8-d^8 dimers are intensely luminescent in acetonitrile solution. In degassed solvent, excitation of $Rh_2(dmb)_4^{2+}$ at 560 nm results in two emission bands with maxima at 663 and >840 nm, respectively (Figure 4). Upon exposure to air, the band at >840 nm disappears, as expected for emission from a triplet state. Transient emission experiments confirm that the 663 nm band decays within the width of an excitation laser pulse (<10 ns), whereas the long-wavelength emission decays with a lifetime of 11.2 μs. In accord with other studies,[7,10,35,36,40,42−49] the emissions are assigned as originating from the spin-allowed and spin-forbidden d$\sigma^*\rightarrow$pσ states, respectively. The fluorescence from $Rh_2(dmb)_2(dppm)_2^{2+}$ maximizes at longer wavelengths (λ_{exc} = 630 nm; λ_{em} = 710 nm) than previously observed for rhodium(I) dimers with bridging diisocyanide ligands, in keeping with this complex's short metal−metal separation.[7,10,35,36,40,42−49] The phosphorescence maximum most likely occurs in the near-infrared region at wavelengths outside the window of our detector. A plot of the emission energy (ν_{em}) vs R^{-3} as in Figure 4 reveals a distinctly more shallow dependence of fluorescence energy maximum on metal−metal separation (ν_{em}, -1×10^2 Å^3 cm^{-1}; ν_{abs}, -6×10^2 Å^3 cm^{-1}), as expected for less variation of Rh−Rh separation for complexes in the Rh−Rh contracted d$\sigma^*\rightarrow$pσ state.

Oxidative Addition of Iodine. The oxidative addition of iodine to $Rh_2(dmb)_4^{2+}$ in room-temperature acetonitrile solution was investigated by absorption spectroscopy (Figure 5a, b). Titration with 1 equiv of I_2 causes the bands attributed to the rhodium(I) complex (560, 318 nm) to lose intensity, while new bands gain intensity (630, 471, 402 nm). The new features at 471 and 402 nm, which are coincident with those of $Rh_2(dmb)_4I_2^{2+}$, grow in intensity with each addition of iodine throughout the titration. In contrast, as expected for a reaction intermediate, the intensity of the 630 nm band maximizes near 0.5 molar equiv of I_2 and loses intensity with further addition of iodine. Under these conditions, addition of 1 equiv does not lead to complete conversion to the diiodo product. After 2 h, the reaction remains incomplete, and there is evidence of additional chemistry as indicated by loss of absorption intensity for bands associated with the d^8-d^8, d^7-d^7, and intermediate species;[50] new features near 290 and

(36) Fordyce, W. A.; Crosby, G. A. *J. Am. Chem. Soc.* **1982**, *104*, 985−988.
(37) Other models dependent on parameter R are possible; we show this particular model because it has been used with success in the quantitative description of stacked d^8 linear-chain systems (Gliemann, G.; Yersin, H. *Struct. Bonding* **1985**, *62*, 87−153. Connick, W. B.; Henling, L. M.; Marsh, R. E.; Gray, H. B. *Inorg. Chem.* **1996**, *35*, 6261−6265.)
(38) Mann, K. R. *Cryst. Struct. Commun.* **1981**, *10*, 451−457.
(39) Smith, D. C.; Miskowski, V. M.; Mason, W. R.; Gray, H. B. *J. Am. Chem. Soc.* **1990**, *112*, 3759−3767.
(40) Miskowski, V. M.; Rice, S. F.; Gray, H. B.; Dallinger, R. F.; Milder, S. J.; Hill, M. G.; Exstrom, C. L.; Mann, K. R. *Inorg. Chem.* **1994**, *33*, 2799−2807.
(41) Stace, J. J.; Connick, W. B. Unpublished results.
(42) Rice, S. F.; Milder, S. J.; Gray, H. B.; Goldbeck, R. A.; Kliger, D. S. *Coord. Chem. Rev.* **1982**, *43*, 349−345.
(43) Dulebohn, J. I.; Ward, D. L.; Nocera, D. G. *J. Am. Chem. Soc.* **1988**, *110*, 4054−4056.
(44) Miskowski, V. M.; Nobinger, G. L.; Kliger, D. S.; Hammond, G. S.; Lewis, N. S.; Mann, K. R.; Gray, H. B. *J. Am. Chem. Soc.* **1978**, *100*, 485−488.
(45) Miskowski, V. M.; Rice, S. F.; Gray, H. B.; Milder, S. J. *J. Phys. Chem.* **1993**, *97*, 4277−4283.
(46) Milder, S. J.; Kliger, D. S.; Butler, L. G.; Gray, H. B. *J. Phys. Chem.* **1986**, *90*, 5567−5570.
(47) Milder, S. J.; Kliger, D. S. *J. Phys. Chem.* **1985**, *89*, 4170−4171.
(48) Milder, S. J.; Goldbeck, R. A.; Kliger, D. S.; Gray, H. B. *J. Am. Chem. Soc.* **1980**, *102*, 6761−6764.
(49) Milder, S. J. *Inorg. Chem.* **1985**, *24*, 3376−3378.
(50) We have found that detailed investigation of this reaction on long time scales is complicated by this apparent degradation chemistry, which is sensitive to light and heat.

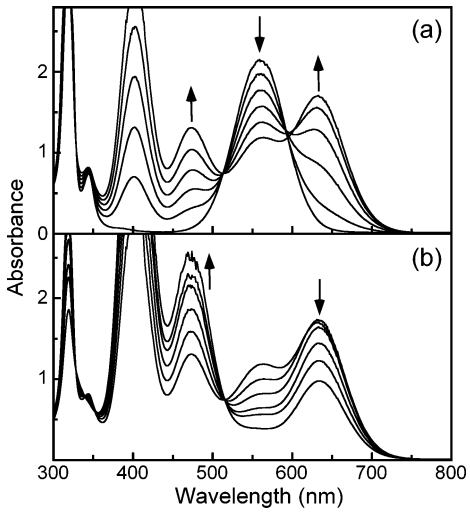

Figure 5. UV−visible absorption spectra of $[Rh_2(dmb)_4](BPh_4)_2$ in acetonitrile solution recorded during addition of (a) 0−0.5 and (b) 0.5−1.0 equiv of iodine in 0.1 molar equiv increments.

360 nm are consistent with formation of I_3^-.[51,52] On the other hand, if excess iodine is used, the reaction is driven to completion.

In dilute solutions (~20 μM dimer), the 630 nm band of the intermediate appears as a weak shoulder; at higher initial concentrations, the maximum intensity approaches or exceeds that of the $Rh_2(dmb)_4^{2+}$ $d\sigma^*\rightarrow p\sigma$ band for the initial solution (Figure 5). This behavior is consistent with formation of a tetramer intermediate composed of two dimers. By analogy to the chemistry of $Rh_2(diprop)_4^{2+}$ in aqueous acid solution,[31,53,54] we suggest that the four metal atoms of the tetramer intermediate are arranged in a linear chain with the two central Rh atoms forming a metal−metal bond.[55] The $CoCl_4^{2-}$ salt of $Rh_4(diprop)_8^{6+}$ has a central Rh−Rh bond length of 2.775(4) Å and outer Rh−Rh distances (2.932(4), 2.923(3) Å) that are intermediate between those of d^7-d^7 and d^8-d^8 dimers.[31] The absorption spectrum of $Rh_4(diprop)_8^{6+}$ also is dominated by a very intense $d\sigma\rightarrow d\sigma^*$ band whose energy varies depending on the donor properties of axial ligands. Notably, the maximum for $Rh_4(diprop)_8I_2^{4+}$ in 1 N H_2SO_4 (622 nm, 166 600 M^{-1} cm^{-1})[54] is remarkably similar to that of the tetramer intermediate formed in the reaction of $Rh_2(dmb)_4^{2+}$ with iodine in acetonitrile solution (630 nm). Additional support for this interpretation comes from the observation that the 630 nm band is thermally sensitive. At 0 °C, the 630 nm band for a 100 μM solution of $Rh_2(dmb)_4^{2+}$ with 0.4 molar equiv of iodine is enhanced in intensity by a factor of >2.7 relative to the room-temperature spectrum; at ~80 °C, the absorption is significantly diminished relative to the room-temperature spectrum.

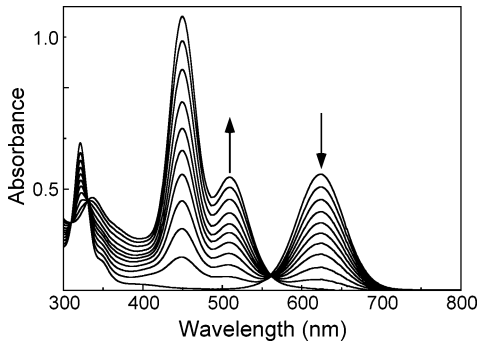

Figure 6. UV−visible absorption spectra of $[Rh_2(dmb)_2(dppm)_2](BPh_4)_2$ in acetonitrile solution recorded during addition of 1.0 equiv of iodine in 0.1 molar equiv increments.

Drastic temperature effects for $Rh_4(diprop)_8Cl_2^{4+}$ have been interpreted in terms of the large Franck−Condon factors that are characteristic of the $d\sigma\rightarrow d\sigma^*$ transition.[54] In the present case, we believe that perturbation of the equilibrium between tetramer and the d^7-d^7/d^8-d^8 dimers, as well as sample degradation at high temperature, contribute to the observed behavior.

The preceding observations are consistent with the following reaction steps:

$$Rh_2(dmb)_4^{2+} + I_2 \rightarrow Rh_2(dmb)_4I^{3+} + I^-$$

$$Rh_2(dmb)_4I^{3+} + I^- \rightarrow Rh_2(dmb)_4I_2^{2+}$$

where the initially formed d^7-d^7 adduct, $Rh_2(dmb)_4I^{2+}$, may have a solvent molecule at the vacant axial position. This species can react rapidly with iodide to form the final diiodo product. Alternatively, it can be intercepted by $Rh_2(dmb)_4^{2+}$ and iodide:

$$Rh_2(dmb)_4I^{2+} + Rh_2(dmb)_4^{2+} + I^- \rightarrow Rh_4(dmb)_8I_2^{4+}$$

The resulting tetramer intermediate reacts with a second equivalent of iodine to give 2 equiv of the diiodo product:

$$Rh_4(dmb)_8I_2^{4+} + I_2 \rightarrow 2Rh_2(dmb)_4I_2^{2+}$$

From the molar absorptivity of $Rh_4(diprop)_8I_2^{4+}$,[54] we estimate that, at the maximum concentration of tetramer observed in the titration depicted in Figure 5, ~10% of the rhodium dimers in solution are in the form of tetramer.

By contrast, titration of $Rh_2(dmb)_2(dppm)_2^{2+}$ with 1 equiv of iodine results in direct conversion to $Rh_2(dmb)_2(dppm)_2I_2^{2+}$ without formation of detectable intermediate (Figure 6). The bands associated with the rhodium(I) complex (321, 624 nm) lose intensity, while the product absorption features at 336, 449, and 509 nm gain intensity. During titration, isobestic points are preserved near 310, 330, and 560 nm; further addition of iodine beyond 1 equiv results in absorption features that are characteristic of iodine in acetonitrile.[52] The spectrum of the product shows an absorption profile (336 (12 000), 449 (35 500), 509 nm (14 600 M^{-1} cm^{-1})) that is remarkably similar to that of $[Rh_2(dmb)_4I_2](PF_6)_2$, but shifted to the red. The two long-wavelength bands are reasonably assigned as strongly coupled $d\sigma\rightarrow d\sigma^*$ and

(51) Popov, A. I.; Swensen, R. F. *J. Am. Chem. Soc.* **1955**, *77*, 3724−3726.
(52) Kebede, Z.; Lindquist, S.-E. *Sol. Energy Mater. Sol. Cells* **1999**, *57*, 259−275.
(53) Sigal, I. S.; Mann, K. R.; Gray, H. B. *J. Am. Chem. Soc.* **1980**, *102*, 7252−7256.
(54) Miskowski, V. M.; Gray, H. B. *Inorg. Chem.* **1987**, *26*, 1108−1112.
(55) While monitoring the iodine reaction by ^1H NMR spectroscopy, we have observed singlet resonances at 4.10 and 4.07 nm that are tentatively assigned to the inequivalent methylene protons of the tetramer.

LMCT transitions. We conclude that the strikingly different reactivities of $Rh_2(dmb)_4^{2+}$ and $Rh_2(dmb)_2(dppm)_2^{2+}$ toward iodine are consistent with the suggestion of Hill and Mann that the steric constraints of the dppm ligands of diisocyanide-bridged rhodium dimers can interfere with association of dimers by metal−metal interactions.[12]

Acknowledgment. We thank Professors M. J. Baldwin and R. Elder, as well as Drs. E. Brooks, S. Macha, and L. Sallans, for expert technical assistance and helpful discussions. Diffraction data were collected through the Ohio Crystallographic Consortium, funded by the Ohio Board of Regents 1995 Investment Fund (CAP-075) and located at the University of Toledo, Instrumentation Center, in A&S, Toledo, OH 43606. W.B.C. thanks the Arnold and Mabel Beckman Foundation for a Young Investigator Award. We thank the National Science Foundation (CHE-0134975) and the University of Cincinnati for generous support of this research.

Supporting Information Available: Crystallographic data, structure refinement details, atomic coordinates, interatomic distances and angles, anisotropic displacement parameters, and calculated hydrogen parameters in CIF format. This material is available free of charge via the Internet at http://pubs.acs.org.

IC060923G